

Flexible Epineural Strip Electrode for Recording in Fine Nerves

Sanghoon Lee, Shih-Cheng Yen, Swathi Sheshadri, Ignacio Delgado-Martinez, Ning Xue, Zhuolin Xiang, Nitish V. Thakor, *Fellow, IEEE*, and Chengkuo Lee*, *Member, IEEE*

Abstract—This paper demonstrates flexible epineural strip electrodes (FLESE) for recording from small nerves. Small strip-shaped FLESE enables us to easily and closely stick on various sized nerves for less damage in a nerve and optimal recording quality. In addition, in order to enhance the neural interface, the gold electrode contacts were coated with carbon nanotubes, which reduced the impedance of the electrodes. We used the FLESEs to record electrically elicited nerve signals (compound neural action potentials) from the sciatic nerve in rats. Bipolar and differential bipolar configurations for the recording were investigated to optimize the recording configuration of the FLESEs. The successful results from differential bipolar recordings showed that the total length of FLESEs could be further reduced, maintaining the maximum recording ability, which would be beneficial for recording in very fine nerves. Our results demonstrate that new concept of FLESEs could play an important role in electroceuticals in near future.

Index Terms—Bipolar configuration, carbon nanotube (CNT), flexible neural electrodes, neural signal recording, polyimide.

I. INTRODUCTION

A GROWING field of electrophysiology research involves finding a reliable way to record tiny neural signals that travel through peripheral nerves or for selective stimulation of these nerves. For instance, bionic limbs may be controlled by using recordings from motor nerves in the peripheral nervous system (PNS), and sensory feedback can then/subsequently be provided by stimulating the sensory nerves [1]. Other emerging applications include achieving therapeutic effects that control chronic diseases through the modulation of electrical signaling patterns in visceral nerves to affect organ systems. This emerging field has been called “electroceuticals” wherein the

Manuscript received April 16, 2015; revised July 18, 2015; accepted July 29, 2015. Date of publication August 11, 2015; date of current version February 16, 2016. This work was supported by grants from the National Research Foundation CRP Project “Peripheral Nerve Prostheses: A Paradigm Shift in Restoring Dexterous Limb Function” (R-719-000-001-281). *Asterisk indicates corresponding author.*

S. Lee, S.-C. Yen, S. Sheshadri, and Z. Xiang are with the Singapore Institute for Neurotechnology, National University of Singapore.

I. Delgado-Martinez was with the Singapore Institute for Neurotechnology, University of Singapore. He is now with the Institute of Neurosciences, Universitat Autònoma de Barcelona and CIBERNED.

N. Xue is with the Institute of Microelectronics, Agency for Science, Technology and Research.

N. V. Thakor is with the Singapore Institute for Neurotechnology, National University of Singapore, and also with the Johns Hopkins University.

*C. Lee is with the Department of Electrical and Computer Engineering and the Singapore Institute for Neurotechnology, National University of Singapore, 117456 Singapore (e-mail: elelc@nus.edu.sg).

Color versions of one or more of the figures in this paper are available online at <http://ieeexplore.ieee.org>.

Digital Object Identifier 10.1109/TBME.2015.2466442

functional stimulation of visceral nerves, such as phrenic nerve and vagus nerve for treating bladder dysfunctions cardiac or enteric control, respectively [2]–[5]. Accordingly, the bidirectional control of the PNS will be at the center of these advances. Due to many physiological and anatomical difficulties to access small nerves, however, the precision acquisition and modulation of electrical signal in PNS has proven to be a challenge. Accordingly, various types of neural electrodes have been reported in the past, such as extraneural (Cuff, FINE) [6]–[9], intrafascicular (LIFE and TIME) [10]–[12] penetrating (USEA) [13]–[15], and regenerative electrodes (SIEVE) [16]–[22]. These electrodes reveal the tradeoffs between high selectivity and low invasiveness. Even though LIFE and TIME show a higher level of selectivity for stimulation by implantation inside nerves, the intrafascicular approach itself can potentially cause nerve damage [23]. On the other hand, extraneural electrodes, such as a spiral cuff and FINE show effective selectivity for stimulation that is similar to acute trials with intrafascicular electrodes [9]. When it comes to recording, however, the low signal-to-noise ratio (SNR) is a major challenge of the cuff-type electrodes, since tight cuff for achieving close contact to a nerve causes eventual nerve damage [6]. In addition, a long length (at least 20 mm) of cuff is usually required for recording high-amplitude signal when tripolar configuration of recording is used [24]. There are limitations of this long-length cuff type: 1) increasing foreign body response exposing longer areas of interfaces between a device and a nerve, which results in changing the functionality of implanted electrodes, such as changes in signal to SNR and decreases in the selectivity [25]; 2) unstable and unreliable device performance due to biomechanical issues resulting from contraction and expansion of the near muscles as a result of relevant movements [26]; 3) difficulty of implanting in very fine nerves that are close to visceral organs and dense tissue networks providing limited surgical and implantation space. Some solutions, such as parylene-based new cuff designs have been proposed for flexible and conformable contact on nerves [27], [28], there is still challenge in applying these to very fine nerves (50–200 μm), such as branches of sciatic nerve, splanchnic, bladder, and vagus nerves that are currently getting attention for bioelectronic medicine. Therefore, developing new electrode design concepts is still desirable for advanced neural electrodes.

This paper proposes a flexible epineural strip electrode (FLESE) that closely sticks to a nerve without undue pressure. The FLESE has small size of strip-shaped body with three electrodes, which allows placing it longitudinally on various sizes of nerves, very much like band aid. Flexible and biocompatible polyimide is used as a body material. In addition, the three

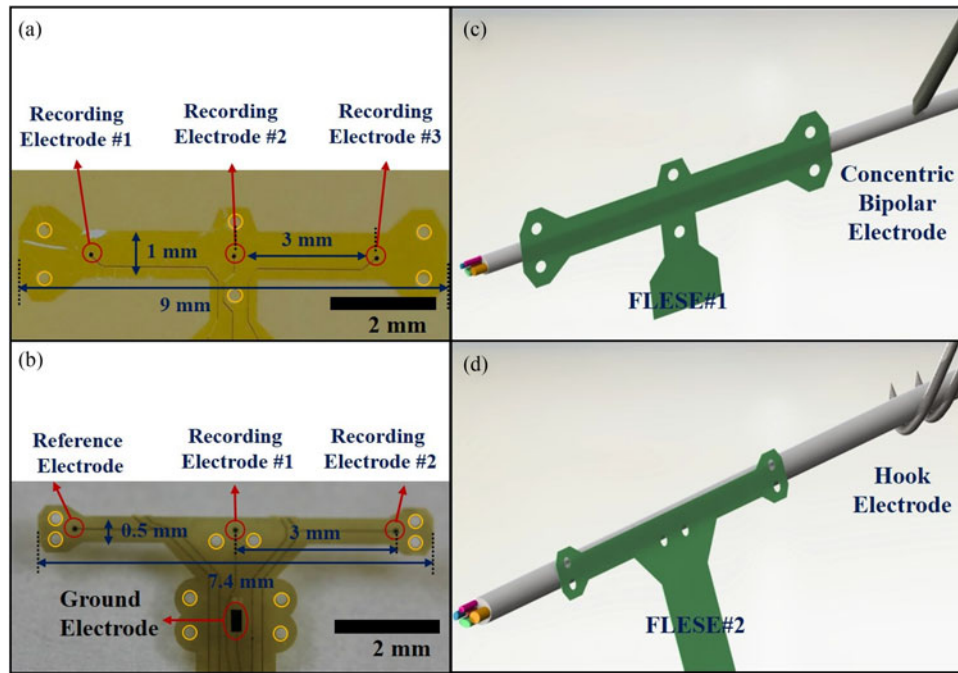


Fig. 1. Pictures of (a) FLESE#1 and (b) FLESE#2. Yellow circles indicate suturing holes for implantation on nerves. Schematic diagrams of configuration of implantations on a nerve, respectively, (c) FLESE#1 with a concentric bipolar electrode, and (d) FLESE#2 with a hook electrode.

sensing electrode metal contacts are coated with carbon nanotube (CNT) in order to reduce the interfacial impedance, as well as to improve the adhesion properties [29]–[34]. Electrically elicited neural signals, elicited by different stimulation electrodes, are recorded by different two designs of FLESEs from main sciatic nerves of rats in order to investigate the feasibility of FLESEs.

II. METHODS

A. Device Design

The FESEs have very small strip-shaped body fabricated from flexible and biocompatible polyimide. This design enables a longitudinal implant on various sizes of thin nerves in a manner analogous to attaching a band aid. This novel design reduces significant nerve damage by just attaching the electrode to the nerve instead of wrapping or penetrating the nerve, while providing direct contact between the nerve and the metal sensors. Another advantage is that the various nerve sizes have little effect on the size of the electrode; in contrast, for a cuff electrode, the inner diameter of a nerve cuff has to be closely matched to the size of the nerve. Thus, the FLESE design allows implanting on very fine nerves with 100 s of micrometer diameter. The electrode has a smooth geometry that prevents nerve trauma from sharp edges. Two different designs are investigated. Both have three sensing electrodes, where the diameter is 100 μm and each distance between the electrodes is 3 mm. To secure the electrode strip to nerves, several suture holes are located on the strip. Surgeons can use the holes to gently suture the electrode directly to the nerve bundle, through the epineurium. Initial design [see FLESE#1 in Fig. 1(a)] has 9 mm length and 1 mm width of strip. The second design [see FESE#2 in Fig. 1(b)] has

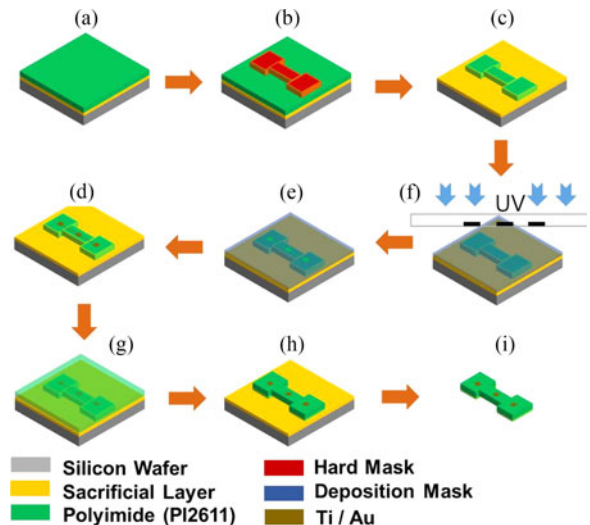


Fig. 2. Fabrication process for FLESEs.

7.5 mm length and 0.5 mm width of strip, as well as a ground round electrode on a longer body. These designs can, of course, be adapted to different nerve sizes and shapes.

B. Device Fabrication

FLESEs are made of two layers of the polyimide with gold sandwiched in between in strip-shape geometry. First, a 1- μm Aluminum (Al) sacrificial layer was deposited on a silicon substrate, then a 6- μm polyimide (PI2611-HD-Microsystems) was spin coated and hard cured under 300 $^{\circ}\text{C}$ for 30 min at a 4- $^{\circ}\text{C}/\text{min}$ ramping rate [see Fig. 2(a)]. After deposition of 200-nm Al as a hard mask, the bottom polyimide structure was patterned on the thin-Al surface after the first lithography step [see Fig. 2(b)].

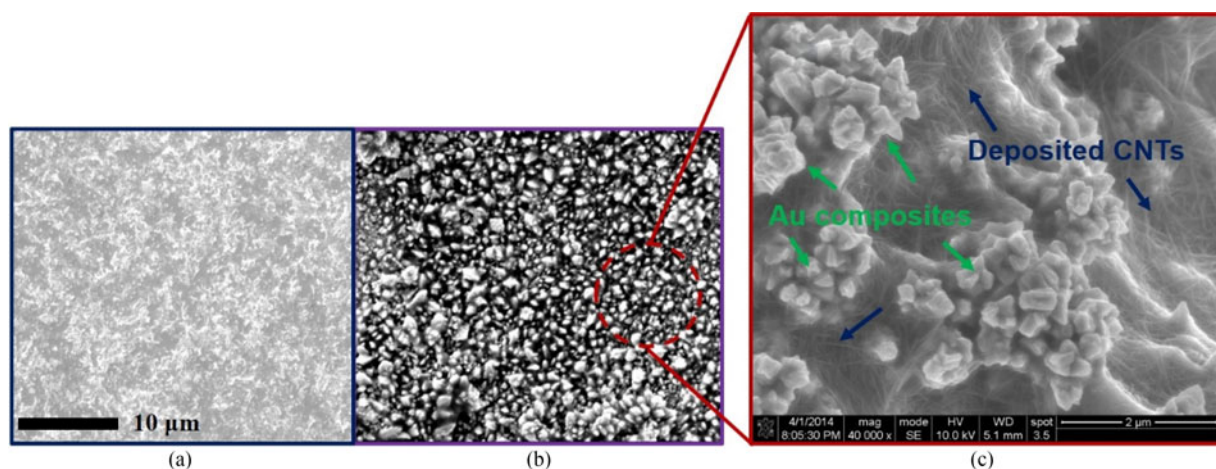


Fig. 3. SEM images (a) before and (b) after CNT coating on electrodes. (c) Magnified SEM images after CNT coating.

Afterward, the exposed polyimide was etched out by a reactive plasma etching process (O_2 gas flow 50 sccm and CF_4 gas flow 10 sccm, RF power 150 W), the remaining Al layer was removed [see Fig. 2(c)]. Layers of Titanium (Ti) (20 nm), and gold (Au) (300 nm) metal electrodes, traces, and pads were subsequently deposited and patterned by a metal evaporation and lift-off process [see Fig. 2(d)–(f)]. Next, a second layer of 6- μm polyimide was coated and fully cured at 350 °C for 30 min [see Fig. 2(g)]. Using the same process as the first polyimide layer patterning, the second polyimide layer was etched and the final structure was formed [see Fig. 2(h)].

C. Device Releasing

The polyimide chip was released from the aluminum sacrificial etching using an electrochemical anodic dissolution process that is often used for metal refining and metal etching [see Fig. 2(i)]. The Al-sacrificial layer on silicon substrate was bonded with copper wire extension encapsulating by nonconductive glue. Then, a platinum (Pt) mesh electrode as an inert electrode put together into a glass beaker of 0.5-M NaCl solution with gentle magnetic stirring. Voltages were applied to the Pt electrode as cathode and the copper wire as anode. The voltage was set below 1 V to avoid O_2 formation at the anode. While applying the voltage, the Al electrode is dissolved into the electrolyte in the form of Al^{3+} or Al_2O_3 by oxidation and H_2 gases released from the Pt surface by H^+ reduction. Once the electrodes were released from the substrate, they were rinsed with 5% HCl acid to remove the suspended Al_2O_3 on the device surface.

D. Electrode Packaging

Pads on the FESEs electrodes were initially designed to match the FPC connectors (Hirose Electric Co. Ltd.) so that the pads were easily inserted with spacer into the connectors and connected by just clicking on them. The connectors avoided damage to the thin-film electrodes during soldering and from tethering force possibly applied during the *in vivo* experiments. The FPC connector was soldered to omnetic cables encapsulated with flexible and biocompatible silicon tube. Insulating UV epoxy

(Vitrilit 4731 VT, Panacol-Elosol GmbH, Daimlerstr) was applied on each connection part to protect components mechanically as well as electrically from *in vivo* environment.

E. Coating of the Electrode Site (Au-CNT Nanocomposites)

CNTs has drawn the great interest by researcher due to its excellent mechanical property, superior charge storage capacity, lower impedance, and neurocompatibility [35]. Also, randomly oriented multiwall CNTs (MWCNTs) enables intimate contact with neurons and cells [30], [31]. Furthermore, CNT coating by an electroplating method provides fabrication simplicity.

For the preparation of CNTs coating in this study, the MWCNTs (Cheap Tubes Inc., USA, length ~ 0.5 – $2 \mu\text{m}$, outer diameter $< 8 \text{ nm}$) were first dispersed in an Au electrolyte bath (TSG-250, Transene, USA) to form a 1-mg·mL $^{-1}$ aqueous solution. Then, the whole solution was sonicated for 2 h to fully suspend the CNTs in the solution. After that, the packaged FESEs and Au wire were connected to the negative and positive terminals of the power supply, respectively. Both the electrode site and the Au wire were then inserted into the solution. A monophasic voltage pulse (1.1 V, 50% duty cycle, 1 min) was applied from the power source. Au ions in the solution, as well as CNTs which absorbed Au ions, migrated to the negative terminals. After absorbing the electrons from the probe contacts, the Au ions were subsequently deposited onto the surface of the recording contacts. The surface morphology of CNT-coated electrodes was characterized by SEM. Fig. 3 shows SEM images of the electrode before and after the CNT coating. Au nanocomposites mixed with CNTs were formed on the surface demonstrating that CNT-Au nanocomposites were successfully coated on the electrode surface by the CNT coating method. This rough and high porosity of surface coatings provides the increment of electrochemical surface area resulting in drastic decrease of interfacial impedance.

F. Electrochemical Impedance Spectroscopy (EIS) Characterization

Impedance characterization of interfacial layers is of paramount important for the performance of neural recording.

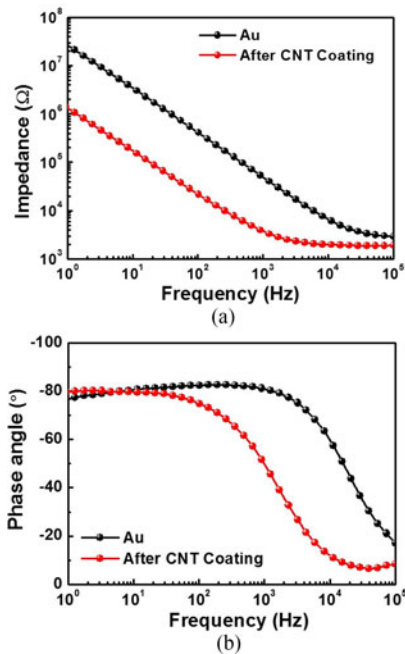


Fig. 4. Results from EIS for (a) the plot of interfacial impedances for with and without CNT coating and (b) the plot of phase angle.

The neural signal will be lost in noisy if the electrode impedance is not low enough [36]. In order to verify the change of interfacial impedances with and without Au-CNT-coated electrodes, EIS was conducted in phosphate buffered saline (PBS, Biowest, pH 7.4, conductivity $\times 1$). The sinusoidal wave with amplitude of 50 mV and frequency spans from 100 kHz to 0.7 Hz was applied. Three electrode configurations with the silver/silver chloride (Ag/AgCl) electrode and a Pt wire as reference and counter electrode, respectively, were used. The output impedance was recorded *in vitro* with an impedance analyzer (Autolab PG-STAT100N voltage potentiostat/galvanostat, Metrohm).

The results of EIS are plotted in Fig. 4. Impedance without CNT coating at 1 kHz was 47 ± 7 k Ω , while the impedance dropped by one order of magnitude (3.6 ± 0.6 k Ω) after deposition of the CNT and Au composites and phase was -48° at 1 kHz. Since high impedance increase signal distortion and reduce SNR, only Au electrodes without CNT coating can not record the high quality of neural signal, while the impedance of electrodes with CNT coating is reasonably low and good for neural signal recording (<10 k Ω).

G. Rat Preparation for In Vivo Test

The experiments were performed in adult female Sprague Dawley rats (250 g) (In Vivos Pte Ltd, Singapore). The rats were acclimatized for one week prior to use in the experiment, with food and water provided *ad libitum* and 12-h lights ON/OFF. The animal care and use procedures conformed to those outlined by the Agri-Food & Veterinary Authority of Singapore, the Institutional Animal Care and Use Committee, and the ethics commission of the National University of Singapore. The animals were anesthetized with a single bolus injection of ketamine/xylazine (150 and 10 mg/kg, respectively, intraperitoneal). After an

adequate depth of anesthesia was attained, the right sciatic nerves were exposed through a gluteal-splitting incision. The FLESEs were placed around the proximal segment of the sciatic nerve. Special care was taken to prevent nerve damage.

H. Physiological Characterization

The neural signals are evoked by electrical stimulation during acute recording tests (studies done under general anaesthesia); evoked activity is used for testing the neural signal recording as well as the calculation of nerve conduction velocity (NCV) [37]. In this study, a sciatic nerve was directly stimulated, and the evoked compound nerve action potentials (CNAPs) were recorded from the sciatic nerve. The nerve was stimulated by the application of a single monophasic 20- μ s pulse, with amplitudes varying between 0.3 and 1.5 mA, using an isolated stimulator box (Digitimer Ltd., UK). This range (6–30 nC/Phase) is acceptable according to the literature [38]. Signals from the implanted FLESEs were acquired using a multichannel amplifier (USB-ME32-FAI System, Multichannel Systems, Inc., USA), at a sampling rate of 50 kHz and a gain of 2000. Data acquisition was done using an MCS system and the data acquisition software (MCRack).

I. Stimulation Electrode and Recording Configuration

A concentric bipolar electrode (Microprobe, Inc.) as a stimulation electrode was implanted proximal to the spinal cord. Bipolar recordings were conducted using three sensing electrodes of FLESE#1 distally placed at about 10 mm distance from the stimulus site. Fig. 5(a) shows the schematic diagram of the implant. The reference electrode was placed in the body in an electrically neutral place. Ground electrode was separately connected to the tail of the rat.

A lab-made hook electrode as another stimulation electrode was implanted at the stimulus site. Differential bipolar recording was conducted indicating that one reference electrode and two sensing electrodes from FLESE#2 were placed on the sciatic nerve. Fig. 5(c) shows the schematic diagram of the implant. The ground electrode on the body of FLESE#2 was contacted to near body.

J. Data Analysis

Electrophysiological data were analyzed using custom-made algorithms in MATLAB (Mathworks, Inc., USA). The NCAPs following the stimulation artifact were identified by the latency of peak as well as the peak–peak amplitude.

III. RESULTS AND DISCUSSIONS

A. In Vivo Recording (FLESE#1 and Bipolar Configuration) Elicited by a Concentric Bipolar Electrode

The FLESE#1 was successfully sutured on a sciatic nerve by microsurgical techniques [see Fig. 5(b)]. Fig. 6(a) shows the recorded CNAP from three different electrodes (E#1, E#2, and E#3) for varying stimulation currents. Each trace corresponds to the average obtained from recording over 50 CNAPs. The

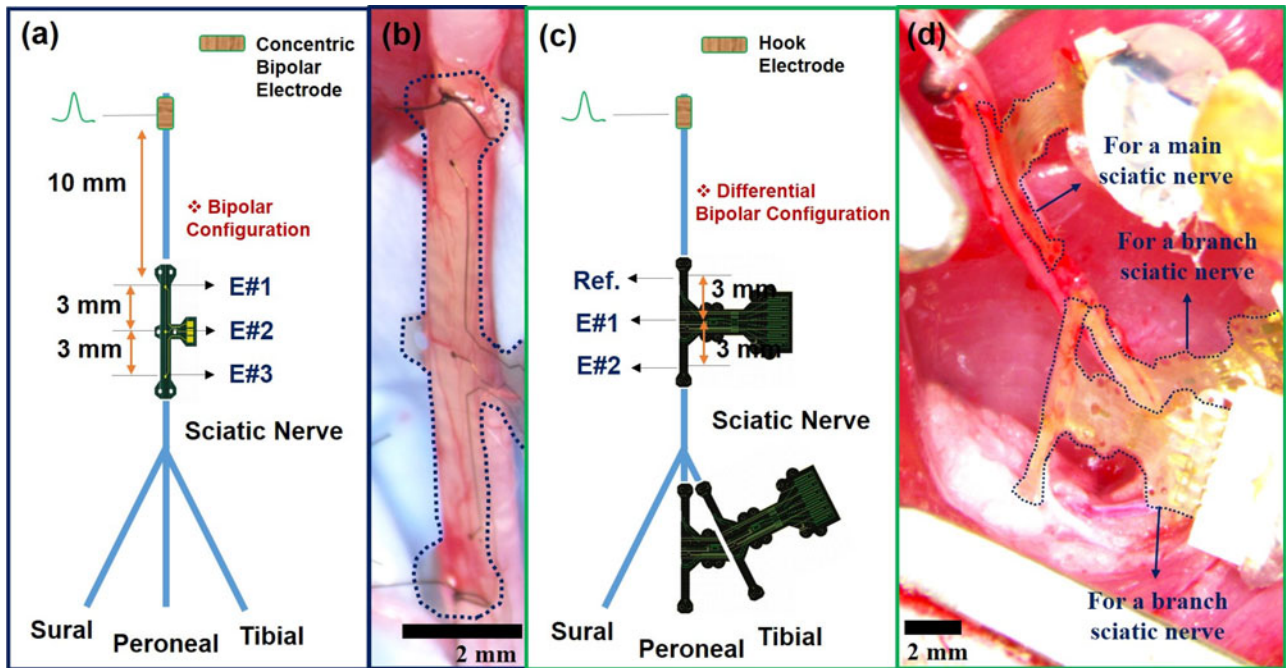


Fig. 5. Schematic diagrams of implanted FLESE#1 (a) and FLESE#2 (c) with the stimulation electrodes. The pictures of implanted FLESE#1 (b) and FLESE#2 (d) on rat sciatic nerves.

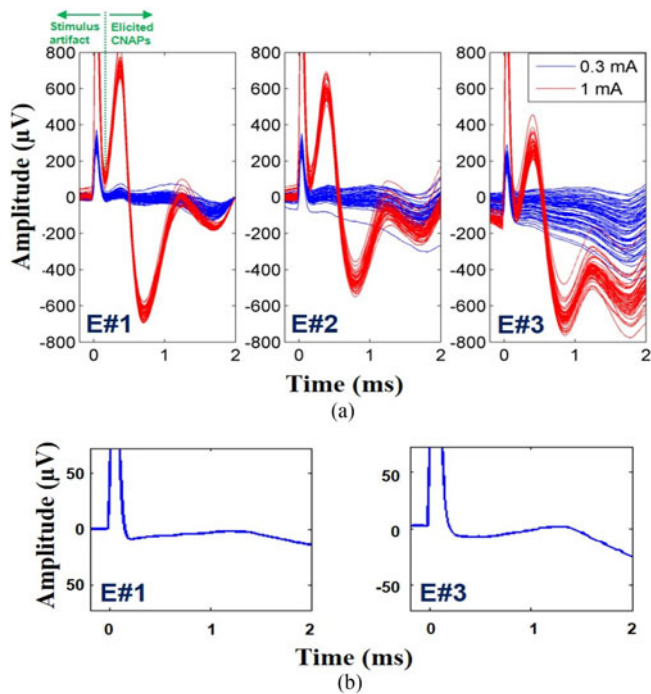


Fig. 6. Results of CNAP recordings of FLESE#1 on a main sciatic nerve elicited by the concentric bipolar electrode (a) before and (b) after applying xylocaine for a nerve block.

CNAPs were recorded following the stimulation artifact: 1) there were no CNAPs of significant amplitude recorded from the electrodes during the stimulation of 0.3 mA, 2) whereas clear and fine neural signals were recorded from the three electrodes at 1 mA, and 3) after the stimulation currents of more than 1 mA, the amplitude of recorded signals did not increase. This

experiment demonstrates that the stimulation current of around 1 mA is the threshold for stimulation of the sciatic nerve by the concentric bipolar electrode. The latency of peak of the CNAP that indicates the time from the onset of the stimulation artifact to the onset of the CNAP was 0.41, 0.42, and 0.44 ms, respectively, from the three electrodes. NCV can be calculated by the below equation [39]:

$$NCV = \Delta x / \Delta t \quad (1)$$

where Δx is the distance that CNAP travels, and Δt is the time that it takes to cover this distance. The calculated NCV is 24–36 m/s. This matches well with the established NCV of the fastest fibers in rat sciatic nerves [40]. The mean amplitude of CNAP from E#1 was $716.15 \pm 39.74 \mu\text{V}$, that of E#2 was $584.28 \pm 42.9 \mu\text{V}$ and that of E#3 was $272.94 \pm 50.55 \mu\text{V}$. This can be attributed to the difference in the distance between the sensing electrodes and the reference electrode.

To verify whether the recorded CNAPs are corrupted by any external noises, such as EMG or the source of stimulation, xylocaine that is normally used for blocking nerve function [41] was applied to the nerve during stimulation with 1-mA current, and CNAP recordings were conducted after 10 min. The result of recorded CNAP after 10 min shows that no signal was recorded except for the stimulus artifact [see Fig. 6(b)]. This demonstrates that the recorded CNAP before blocking nerve is not corrupted. However, the needle-type concentric electrode showed the difficulty of reliable and repeatable implantation since some movements of near muscles during the stimulation made lose its original position as well as repeatable pricking for the same stimulus position cause bleeding the sciatic nerve degrading normal nerve condition.

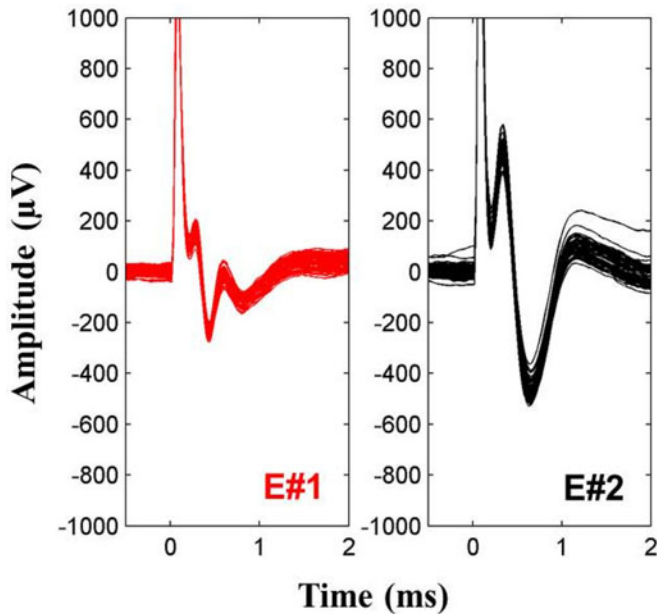


Fig. 7. Results of CNAP recording of FLESE#2 from E#1 and E#2 on a main sciatic nerve elicited by a hook electrode.

B. In Vivo Recording (FLESE#2 and Differential Bipolar Configuration) Elicited by a Hook Electrode

The FLESE#2 has narrower strip body that easily sticks even on the smaller branches of sciatic nerves (the diameters of 0.2–0.3 mm) compared with the FLESE#1. Also, it has longer tail body to the connector so that it allows for a stable implantation by reducing the tethering force. Also, ground electrode is on the tail body so that an additional or separate ground electrodes is not necessary, which again would be desirable for long-term implantation. The FLESE#2s were readily put on the main sciatic nerve and very small branch nerves [see Fig. 5(d)]. Furthermore, they showed good adhesion properties enough to stick the nerves without any suturing during the acute recording procedure. This might be due to the narrow width of the strip body, which reduces noncontact areas, promoting a stronger interface between the strip body and the nerve, as well as CNT's adhesion properties.

Differential bipolar configuration was used for CNAP recording. It is a more effective way for recording in that the activity that is distant from both electrodes appears as common mode to the two recording electrodes, and is rejected, while activity in the immediate vicinity of the two electrode is differential mode and is amplified [24]. Also, the bipolar configuration requires an additional reference electrode put inside the body, which also limits long-term implantation. One sensing electrode on the FLESE#2 was set as a reference electrode and the other two sensing electrodes were set as recording electrodes [see Fig. 5(c)]. Also, the hook electrode was used as the stimulation electrode for more reliable and repeatable stimulation. The stimulation protocol was as described above. Threshold stimulation current was found to be around 1 mA and clear and fine CNAPs were recorded. Fig. 7 shows the result of recorded CNAP ($n = 60$) from the two recording electrodes on the FLESE#2 in a rat

main sciatic nerve elicited by the hook electrode with stimulus current of 1 mA. The mean amplitude of CNAP from E#1 was $235.7 \pm 20.1 \mu\text{V}$ and that from E#2 was $466.1 \pm 34.6 \mu\text{V}$. The difference of amplitude is most likely due to the nature of conduction or organization of axonal fiber/fascicles or placement. Short distances between reference and recording electrodes compensates CNAP resulting in low amplitudes [24]. In the main sciatic nerve, distance gap of 3 mm between the recording electrode #1 and #2 resulted in a $230 \mu\text{V}$ difference. For noise analysis, the mean amplitude of the noise from the electrodes was $12.60 \pm 0.84 \mu\text{V}$, which were identified before and after the CNAP.

IV. CONCLUSION

The FLESEs were proposed and investigated as new concepts for recording from small nerves. The Au-CNTs-coated sensing electrodes showed reasonable interfacial impedance at 1 kHz as well as good adhesion properties on nerves. In addition, there is no risk for applying pressure on nerve that eventually causes nerve damage. Sciatic nerve in a rat was stimulated by using different types of electrodes (a concentric bipolar electrode and a hook electrode), and clear and fine CNAPs were recorded through bipolar or differential bipolar configuration. The FLESE#2 not only showed good adhesion properties enough to implant without suturing during acute recording experiment, but the longer tail body was also beneficial for reducing the tethering force that would be encountered during implantation. In addition, locating a ground electrode on the tail body would be beneficial for long-term implantation with differential bipolar recording. Also, the recorded CNAPs demonstrates that 3 mm distance between reference and recording electrodes for differential bipolar configuration is enough to record clear CNAPs, although the amplitude is lower than with a 6 mm distance. It means that total length of strip body can be reduced further maintaining the maximum recording ability. Overall experimental results demonstrate that FLESE could play an important role in clinical neuroprosthetics and neurotherapeutic technologies in the near future.

REFERENCES

- [1] S. Raspopovic *et al.*, "Restoring natural sensory feedback in real-time bidirectional hand prostheses," *Sci. Transl. Med.*, vol. 6, no. 222, pp. 222ra19, 2014.
- [2] K. Famm *et al.*, "A jump-start for electroceuticals," *Nature*, vol. 496, pp. 159–161, 2013.
- [3] S. Reardon, "Electroceuticals spark interest," *Nature*, vol. 511, pp. 18, 2014.
- [4] R. A. Gaunt and A. Prochazka, "Control of urinary bladder function with devices: Successes and failures," *Prog. Brain Res.*, vol. 152, pp. 163–194, 2006.
- [5] N. Stakenborg *et al.*, "The versatile role of the vagus nerve in the gastrointestinal tract," *EMJ Gastroenterol.*, vol. 1, pp. 106–114, 2013.
- [6] G. C. Naples *et al.*, "A spiral nerve cuff electrode for peripheral nerve stimulation," *IEEE Trans. Biomed. Eng.*, vol. 35, no. 11, pp. 905–916, Nov. 1988.
- [7] J. A. Hoffer and K. Kallesor, *How to Use Nerve Cuffs to Stimulate, Record or Modulate Neural Activity*. Boca Raton, FL, USA: CRC Press, 2001.
- [8] D. J. Tyler and D. M. Durand, "Functionally selective peripheral nerve stimulation with a flat interface nerve electrode," *IEEE Trans. Neural Syst. Rehabil. Eng.*, vol. 10, no. 4, pp. 294–303, Dec. 2002.
- [9] D. W. Tan *et al.*, "A neural interface provides long-term stable natural touch perception," *Sci. Transl. Med.*, vol. 6, pp. 257ra138, 2014.

- [10] N. Lago *et al.*, "Assessment of biocompatibility of chronically implanted polyimide and platinum intrafascicular electrodes," *IEEE Trans. Biomed. Eng.*, vol. 54, no. 2, pp. 281–290, Feb. 2007.
- [11] T. Boretius *et al.*, "A transverse intrafascicular multichannel electrode (TIME) to interface with the peripheral nerve," *Biosens. Bioelectron.*, vol. 26, pp. 62–69, 2010.
- [12] J. Badia *et al.*, "Biocompatibility of chronically implanted transverse intrafascicular multichannel electrode (TIME) in the rat sciatic nerve," *IEEE Trans. BioMed. Eng.*, vol. 58, no. 8, pp. 2324–2332, Aug. 2011.
- [13] M. B. Christensen *et al.*, "The foreign body response to the Utah slant electrode array in the cat sciatic nerve," *Acta Biomaterialia*, vol. 10, pp. 4650–4660, 2014.
- [14] H. A. C. Wark *et al.*, "A new high-density penetrating microelectrode array for recording and stimulating sub-millimeter neuroanatomical structures," *J. Neural. Eng.*, vol. 10, art. no. 045003, pp. 1–10, 2013.
- [15] H. A. C. Wark *et al.*, "Behavioral and cellular consequences of high-electrode count Utah arrays chronically implanted in rat sciatic nerve," *J. Neural. Eng.*, vol. 11, art. no. 046027, pp. 1–13, 2014.
- [16] S. P. Lacour *et al.*, "Polyimide micro-channel arrays for peripheral nerve regenerative implants," *Sens. Actuators A, Phys.*, vol. 147, pp. 456–463, 2008.
- [17] S. P. Lacour *et al.*, "Long micro-channel electrode arrays: A novel type of regenerative peripheral nerve interface," *IEEE Trans. Neural Syst. Rehabil. Eng.*, vol. 17, no. 5, pp. 454–460, Oct. 2009.
- [18] R. Midha, "Emerging techniques for nerve repair: Nerve transfers and nerve guidance tubes," *Clin. Neurosurg.*, vol. 53, pp. 185–190, 2006.
- [19] J. IJkema-Paassen *et al.*, "Transection of peripheral nerves, bridging strategies and effect evaluation," *Biomaterials*, vol. 25, pp. 1583–1592, 2004.
- [20] G. E. Rutkowski *et al.*, "Synergistic effects of micropatterned biodegradable conduits and Schwann cells on sciatic nerve regeneration," *J. Neural Eng.*, vol. 1, pp. 151–157, 2004.
- [21] I. P. Clements *et al.*, "Regenerative scaffold electrodes for peripheral nerve interfacing," *IEEE Trans. Neural Syst. Rehabil. Eng.*, vol. 21, no. 4, pp. 554–566, Jul. 2013.
- [22] J. Scheib and A. Hoke, "Advances in peripheral nerve regeneration," *Nature*, vol. 9, pp. 668–676, 2013.
- [23] G. D. Pino *et al.*, "Invasive neural interfaces: the perspective of the surgeon," *J. Surg. Res.*, vol. 188, pp. 77–87, 2014.
- [24] K. W. Horch and G. S. Dhillon, *Neuroprosthetics: Theory and Practice*, vol. 2. Singapore: World Scientific, 2004.
- [25] B. Hiebl *et al.*, "In vivo assessment of tissue compatibility and functionality of a polyimide cuff electrode for recording afferent peripheral nerve signals," *Appl. Cardiopulmonary Pathophysiol.*, vol. 14, pp. 212–219, 2010.
- [26] S. M. Restaino *et al.*, "Biomechanical and functional variation in rat sciatic nerve following cuff electrode implantation," *J. Neuroeng. Rehabil.* vol. 11, pp.73, 2014.
- [27] H. Yu *et al.*, "A parylene self-locking cuff electrode for peripheral nerve stimulation and recording," *J. Micromech. Microeng.*, vol. 23, pp. 1025–1035, 2014.
- [28] X. Kang *et al.*, "Self-closed parylene cuff electrode for peripheral nerve recording," *J. Microelectromech. Syst.*, vol. 24, pp. 319–332, 2015.
- [29] K. Wang *et al.*, "Neural stimulation with a carbon nanotube microelectrode array," *Nano Lett.*, vol. 6, no. 9, pp. 2043–2048, 2006.
- [30] G. Cellot *et al.*, "Carbon nanotubes might improve neuronal performance by favouring electrical shortcuts," *Nature Nanotechnol.*, vol. 4, pp. 126–133, 2009.
- [31] A. O. Fung *et al.*, "Electrochemical properties and myocyte interaction of carbon nanotube microelectrodes," *Nano Lett.*, vol. 10, pp. 4321–4327, 2010.
- [32] E. W. Keefer *et al.*, "Carbon nanotube coating improves neuronal recordings," *Nature Nanotechnol.*, vol. 3, pp. 434–439, 2008.
- [33] A.O. Lobo *et al.*, "Cell viability and adhesion on as grown multi-wall carbon nanotube films," *Mater. Sci. Eng. C*, vol. 28, no. 2, pp. 264–269, 2008.
- [34] P. Galvan-Garcia *et al.*, "Robust cell migration and neuronal growth on pristine carbon nanotube sheets and yarns," *J. Biomater. Sci. Polymer Ed.*, vol. 10, pp. 1245–1261, 2007.
- [35] S. Minnikanti and N. Peixoto, "Implantable electrodes with carbon nanotube coating," in *Carbon Nanotubes Applications on Electron Devices*. Rijeka, Croatia: InTech, 2011.
- [36] W. Franks *et al.*, "Impedance characterization and modeling of electrodes for biomedical applications," *IEEE Trans. Biomed. Eng.*, vol. 52, no. 7, pp. 1295–1302, Jul. 2005.
- [37] K. S. Mathews *et al.*, "Assessment of rat sciatic nerve function following acute implantation of high density Utah slanted electrode array (25 electrodes/mm²) based on neural recordings and evoked muscle activity," *Muscle Nerve*, vol. 3, pp. 417–424, 2014.
- [38] A. Branner and R. A. Normann, "A multielectrode array for intrafascicular recording and stimulation in sciatic nerve of cats," *Brain Res. Bull.*, vol. 51, pp. 293–306, 2000.
- [39] J. Li *et al.*, "Current distance relationships for peripheral nerve stimulation localization," *Anesthesia Analgesia*, vol. 112, no. 1, pp. 236–241, 2011.
- [40] N. Dalkilic *et al.*, "The effect of tramadol on the rat sciatic nerve conduction: A numerical analysis and conduction velocity distribution study," *Yakgaku Zasshi*, vol. 4, pp. 485–493, 2009.
- [41] J. G. Thalhammer *et al.*, "Neurologic evaluation of the rat during sciatic nerve block with lidocaine," *Anesthesiology*, vol. 4, pp. 1013–1025, 1995.

Authors' photographs and biographies not available at the time of publication.